Astron. Astrophys. 324, 1027–1035 (1997)

ASTRONOMY
AND
ASTROPHYSICS

The EUV spectrum of κ Ceti: an active Sun

E. Landi[1], **M. Landini**[1], **and G. Del Zanna**[2]

[1] Department of Astronomy and Space Science, University of Florence, Italy
[2] Center for Astrophysics, Un. of Central Lanscashire, Preston, UK

Received 12 December 1996 / Accepted 3 March 1997

Abstract. The spectrum of κ Cet in the region 80 -370 Å observed by EUVE Spectrometers is analyzed to investigate the transition region and the corona of the star. The star appears to be in a rather quiet condition and no evidence exists of flare-like lines observed in many active stars. Several emission lines of moderately ionized iron (from Fe IX to Fe XVIII) are identified and used together with I.U.E. observations to evaluate the $differential\ emission\ measure$ (DEM). The DEM peaks at about $3 \cdot 10^6 K$, a value typical of solar active regions. This is confirmed by a comparison with the spectrum of an Active Region of the Solar Corona measured by the Coronal Diagnostic Spectrometer on SOHO showing very similar features.

Key words: stars: individual: κ Ceti – stars: coronae – stars: late-type – ultraviolett: stars

1. Introduction

κ Ceti (HD 20630 G5 V) is a solar like star well known since a long time for its chromospheric and coronal activity.

Strong emission in Ca II was detected by Wilson and Bappu in 1957, who classified the star as one of the first dwarfs showing chromospheric activity, later confirmed by remarkable intensity of h and k emission lines of magnesium (Rego and Fernández-Figueroa, 1979) The detection of He I line 10830 A, by Zirin (1976) was clear evidence that a transition region and a corona surrounded the star. Strong flare activity has also been reported (Robinson and Bopp, 1987) showing He I 5876 Å, in emission for half an hour, well correlated with enhanced Ca II radiation.

Repeated measurements of the Ca II line fluxes are available (e.g. Rutten 1987) and the fluxes of other chromospheric lines (e.g. Mg II) and transition region lines have been obtained with IUE (Rego et al. 1980). The latter spectra have been modeled by Fernández-Figueroa et al. (1981) and de Castro et al. (1981) and from density sensitive line ratios an electron pressure of $\sim 10^{16}$ cm^{-3} K has been estimated. The star has also been observed with the Einstein Observatory and EXOSAT. Schmitt et al. (1987) compare these observations and find that the average temperatures and emission measures agree to within a factor of two. Einstein, EXOSAT and IUE observations have been used to model a multitemperature differential emission measure distribution and to infer constraints on the energy balance in the outer atmosphere of the star (Monsignori Fossi et al., 1986).

Further indication of magnetic activity has been given by Saar (1987), who finds magnetic field B_s = 1500 Gauss and filling factors f_s = 0.35. Variations in $B_s f_s$ over the stellar cycle of about 30% have been found by Saar (1990) and Saar and Baliunas (1992), and are presumably caused by the presence of active regions.

Models of transition regions of solar like stars, similar to K Cet, have been extensively studied by Jordan (1969,1992), Landini et al. (1985), and Jordan et al. (1986,1991) with the aim to have some insight in the problem of heating their high temperature outer atmospheres.

All the information concerning the coronal model have been supplied by instruments with very poor spectral resolution (Pallavicini et al. 1988). The EUVE Spectrometers offers the unique possibility to detect single line emission and investigate the differential emission measure with high temperature detail.

The star is slightly smaller then the Sun (R_*/R_o = 0.93) and lies 9.3 pc from the Earth; to take into account of the interstellar medium absorption, the assumed column density is $Log(NH)$ = 18.3 cm^{-2}.

In Sect. 2. the observations, obtained during the EUVE Guest Observing Programm 1994 by Monsignori Fossi, so early deceased, and C. Jordan, are described and data reduction is discussed ; in Sect. 3. the line identification and the differential emission measure procedure is presented; in Sect. 4. the DEM is used to evaluate a synthetic spectrum and look for a few more lines identification; in Sect. 5. a comparison with the spectrum of a moderately active region measured by the Coronal Diagnostic Spectrometer (C.D.S.) on SOHO is performed showing that K Cet appears to be very similar to the Sun.

2. Observation and data reduction

κ Cet was observed with the EUVE spectrometers (Bowyer and Malina 1991) covering the short (70-190 Å , SW), medium

Send offprint requests to: E. Landi

(140-380 Å, MW) and long (280-760 Å, LW) extreme ultraviolet wavelengths with a spectral resolution of $\Delta\lambda \approx 0.5$, 1 and 2 Å respectively. The observation lasted from October,12,1994, $02^h53^mU.T.$ to October,14,1994, $19^h41^mU.T.$

The SW, MW and LW raw spectra in the form of QPOE (Quick Position Ordered) files have been analyzed with the EUVE Guest Observer Center package (1995) which consists of a calibration database and relative software. Other standard spectroscopic IRAF tasks have also been used to extract the spectra. The one-dimensional spectra were extracted, subtracting an average background selected in two regions of the detector, above and below the spectrum. Corrections for electronics dead time and limited telemetry allocation (known as "Primbsching") were also applied to the data.

The final exposure times in seconds were 127966 s for SW section, 130328 s, (MW) and 125482 s (LW).

Line fluxes were obtained using a standard IRAF routine adopted for EUVE spectra reduction; the selected spectral interval is fitted with gaussian line profiles with fixed FWHM (different in each channel) and a linear continuum; the signal-to-noise ratio was calculated over 7 pixels (the resolution of the three channels) and used to evaluate the uncertainty on the measured fluxes.

The resulting wavelength calibrated spectra for SW, MW and LW channels, corrected with the detector effective areas, are reported in Figs. 1, 3 and 4.

The exposure times were sufficient for a rather strong detection of some of the most prominent features of a quiet corona despite the interstellar attenuation in all the three channels.

The signal-to-noise ratio (S/N) was calculated over 7 pixels, equivalent to the resolution of the three channels. The S/N ratio has been calculated as follows

$$\mathrm{SNR}(\lambda) = \frac{S_\lambda}{\sigma(\lambda)} = \frac{S_\lambda}{\sqrt{(S_\lambda + \overline{B_\lambda}(1 + H_B/H_{sp}))}},$$

where $\sigma(\lambda)$ is the standard deviation of the flux measurement, S represents the signal from the target, $\overline{B}$ is the average background subtracted from the total counts, and H_{sp} and H_B are, respectively, the width of the extraction window for the spectrum and for the background in the direction perpendicular to the dispersion. The resulting values have been used to evaluate the uncertainties on the measured fluxes, and allow to identify well detected lines.

3. The analysis of κ Ceti spectrum

The observed spectrum of κ Cet resulting from the data reduction shows strong detection for a few spectral lines (with a Signal-to-noise ratio greater than 3) especially for the Medium Wavelength (MW) detector. The Long Wavelength (LW) channel shows a very confused spectrum for wavelengths greater than 550 Å. However no strong lines are detected longward of 370 Å . The noise level of the Short Wavelength channel allows only few lines to be identified with confidence. A list of the identified lines is given in Table 1, together with the observed flux corrected for interstellar absorption and the temperature of maximum abundance for the ion they belong to.

Table 1. Measured fluxes of κ Cet at Earth from EUVE and IUE. Fluxes are corrected for the interstellar absorption.

Ion	λ_{obs} (Å)	Flux (ph cm^{-2} s^{-1})	Log T	Detector
Fe XVIII	93.92	$(2.0 \pm 0.5)\ 10^{-4}$	6.8	S.W.
Fe XIX	108.37	$(1.3 \pm 0.4)\ 10^{-4}$	6.9	S.W.
Fe IX	171.07	$(4.9 \pm 2.3)\ 10^{-4}$	5.8	S.W.
	171.07	$(5.5 \pm 1.8)\ 10^{-4}$	5.8	M.W.
Fe X	174.53	$(5.9 \pm 2.7)\ 10^{-4}$	5.9	S.W.
	174.53	$(9.6 \pm 3.3)\ 10^{-4}$	5.9	M.W.
Fe XII	192.92	$(9.7 \pm 3.2)\ 10^{-4}$	6.1	M.W.
Fe XIV	220.09	$(1.3 \pm 0.4)\ 10^{-3}$	6.3	M.W.
He II	256.32	$(1.6 \pm 0.6)\ 10^{-3}$	4.7	M.W.
Fe XV	284.16	$(8.3 \pm 0.9)\ 10^{-3}$	6.3	M.W.
He II	303.78	$(9.8 \pm 1.7)\ 10^{-3}$	4.7	M.W.
	303.78	$(7.3 \pm 1.2)\ 10^{-3}$	4.7	L.W.
Fe XVI	335.41	$(1.4 \pm 0.2)\ 10^{-2}$	6.4	M.W.
	335.41	$(1.1 \pm 0.1)\ 10^{-2}$	6.4	L.W.
Fe XVI	360.76	$(6.6 \pm 1.1)\ 10^{-3}$	6.4	M.W.
	360.76	$(9.5 \pm 1.2)\ 10^{-3}$	6.4	L.W.
N V	1243	$(4.2 \pm 1.1)\ 10^{-3}$	5.3	IUE
C II	1335	$(1.8 \pm 0.5)\ 10^{-2}$	4.4	IUE
C IV	1551	$(3.2 \pm 0.8)\ 10^{-2}$	5.0	IUE
C I	1657	$(6.1 \pm 1.5)\ 10^{-2}$	4.0	IUE
O I	1303	$(1.3 \pm 0.3)\ 10^{-2}$	4.0	IUE
Si IV	1397	$(1.8 \pm 0.4)\ 10^{-2}$	5.1	IUE
Si II	1814	$(6.7 \pm 1.7)\ 10^{-2}$	4.3	IUE

It is evident that these lines are formed in a rather quiet corona, since the typical features of a flare spectrum (i.e. Fe XXIV 192.04 Å, Fe XXII 128.7 Å, Fe XXII 135.8 Å) (Monsignori Fossi et al. 1995a) are absent, while the listed lines are normally seen in the spectra of the quiet Sun. One of the *hottest* lines usually seen in active stars, the blend Fe XXIII + Fe XX 132.83, is not detected and only an upper limit is used in order to put some constraint to the behavior of the Differential Emission Measure for temperatures greater than 10^7 K. The two lines 256.32 Å and 303.78 Å are emitted by the lower and cooler transition region and belong to the spectrum of He II whose maximum abundance temperature is $10^{4.7}$ K.

Since we are interested in deriving a model for the Differential Emission Measure over the Transition Region as well as the corona of κ Cet, we have complemented the EUVE identified line list with other lines observed by IUE. The adopted fluxes for these lines come from Oranje (1986) and belong to transitions of ions whose maximum temperature abundance ranges from $10^{4.7}$ to $10^{5.6}$ K. The fluxes of these lines have been derived by the author directly from the IUE flux numbers FN found in the literature, correcting the published data for different calibrations. The errors associated to the measured fluxes were assumed to be 25 %, as specified in the paper. Since both the EUVE and IUE lines are emitted during quiescent phases of the atmosphere of κ Cet their observed fluxes should be directly comparable and

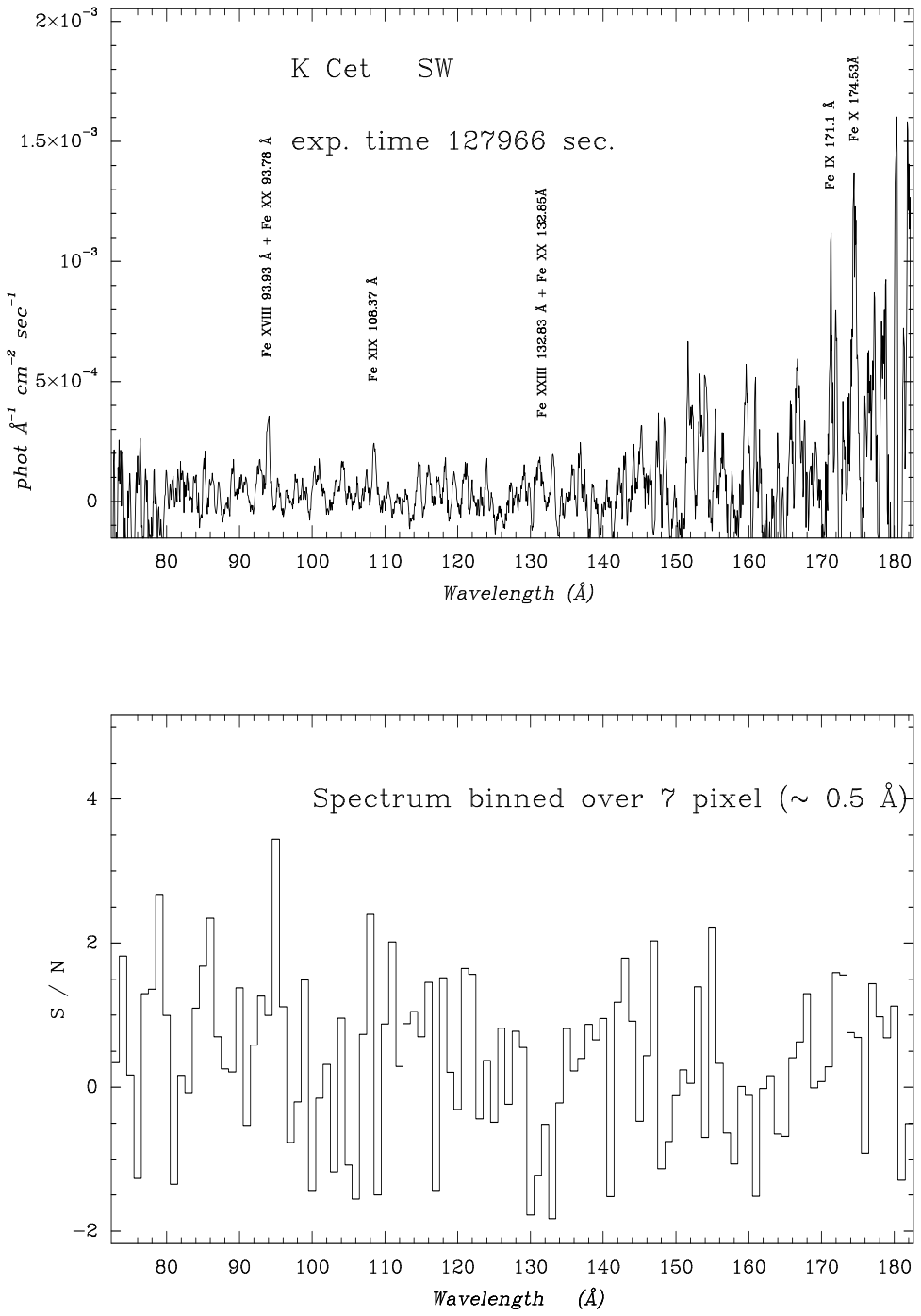

Fig. 1. The SW observed spectrum (top) and the Signal-to-Noise ratio (bottom) plotted versus wavelength

can be used to derive a DEM model for the Transition Region and the Corona of the star.

It is worth noting that some of the observed lines listed in Table 1 have been detected in two of the three channels: Fe IX 171.07 Å and Fe X 174.53 Å in the SW and MW detectors, He II 303.78 Å and Fe XVI 335.41 and 360.76 Å in MW and LW channels. Both values are listed in Table 1.

3.1. The synthetic spectrum

The intensity of a spectral line ($i \rightarrow j$) for an optically thin coronal plasma is given by:

$$(1) \qquad I_{ij} = K Ab(Z) e^{-\sigma(\lambda) N_H} \int_V G_{ij}(T, N_e) N_e^2 dV =$$

$$= K\ Ab(Z)\ e^{-\sigma(\lambda) N_H} \int_T G_{ij}(T, N_e) f(T) dT \quad ph\ cm^{-2}\ s^{-1}$$

where

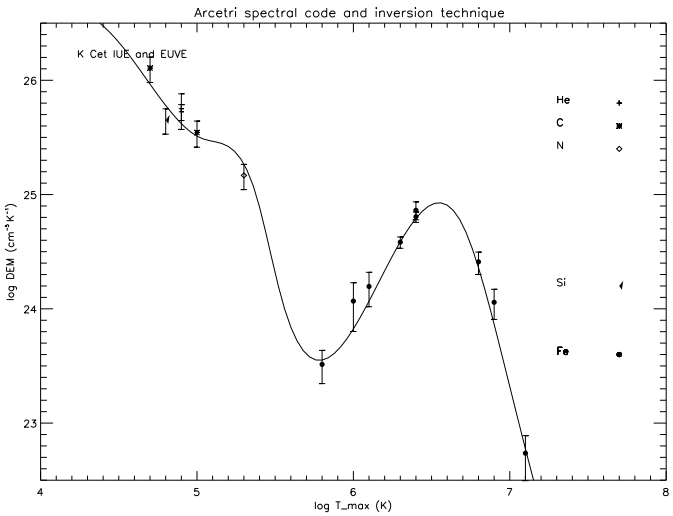

Fig. 2. Differential Emission Measure for K Cet using IUE and EUVE lines

- K is a constant which takes into account the properties of the instruments and the star distance;
- Ab(Z) is the abundance of element Z relative to H;
- f(T) = N_e^2 (dV/dT) is the Differential Emission Measure;
- $N_H = \int n_H dh$ is the hydrogen column density between the star and the Earth;
- $\sigma(\lambda)$ is the absorption cross section of the interstellar medium;
- $G_{ij}(T, N_e)$ is a function of the line atomic data and depend on the electron temperature (T) mainly through the ion abundance, and on the electron density (N_e), mainly through the level population.

To evaluate the $G_{ij}(T, N_e)$ functions we have made use of a version of the Arcetri spectral code (Landini and Monsignori Fossi 1990, Monsignori Fossi and Landini 1994 b) which has been updated using the new extensive database CHIANTI (Dere et al. 1996). This new version of the Arcetri spectral code will be soon released (Landi and Landini 1997) and includes:

- The calculation of the level population and $G_{ij}(T, N_e)$ functions under the assumption of statistical equilibrium for the most important ions of the isoelectronic sequences of Li, Be, B, C, N, O, F, Ne, Na Mg, and for the Iron ions from Fe VII to Fe XXIV. The atomic data necessary to perform the calculation are taken from the CHIANTI database.
- The evaluation of the $G_{ij}(T, N_e)$ functions for lines of isoelectronic sequences of H, He, Al, Ar, Cl, F, K, P, Si not included in the CHIANTI database. Assumption is made that the population of the upper level occurs via collisional excitation from ground level only.
- The evaluation of the ionization balance for Fe ions of Arnaud and Raymond (1992), together with an updating for the other elements made by Landini and Monsignori Fossi (1991)
- Free-free, free-bound and two-photon emission continuum

The column density N_H in the direction of κ Cet is assumed to be 2 10^{18} cm^{-2} using a mean hydrogen density of 0.07 cm^{-3} (Paresce, 1984); a He I/ H I ratio of 0.1 and He II/ H I ratio of 0.01 have been assumed. In order to take into account the interstellar absorption the ISM photoionization cross sections of Rumph et al (1994) were adopted. The assumed column density N_H is in agreement with the observed ratio of the two Fe XVI 335 and 360 lines, that is very sensitive to the column density N_H in the range 10^{18} - 10^{19} cm^{-2}.

Unfortunately it is not possible to use the intensity ratio technique to determine the mean electron density N_e of the emitting plasma since no couples of density sensitive lines of the same ion are available in the observed spectrum. Nevertheless we are confident that the electron density should not be greater than 3 10^9 cm^{-3} since for higher values other spectral lines (Fe XIII 203.8 lines) should have been detected, and Fe XII 192 line should have been much weaker than observed. The adopted electron density is therefore 10^9 cm^{-3}.

3.2. The intensity integral inversion procedure and the DEM determination

Information on the DEM model f(T) may be derived by combining measurements of the fluxes for set of m spectral lines with the knowledge of the appropriate contribution functions G_{ij}. The numerical procedure we have used to evaluate the DEM function f(T) is an application of the "maximum entropy method", described by Monsignori Fossi and Landini (1991a,b).

The f(T) function is assumed to be a cubic spline function with n (few) selected reference points T_i for which the proper $f_i = f(T_i)$ is specified. When f_i change, the function to be optimized is (Jeffrey and Rosner,1986):

$$F = S + \lambda\ \chi^2$$

with

$$\chi^2 = \frac{\Sigma_s (I_{ex,s} - I_{ob,s})^2}{\sigma_s^2} \qquad for\ s = 1, ..., m$$

$$S = \Sigma_i f_i\ ln\ \frac{f_i}{w_i} \qquad entropy\ of\ the\ information\ < f >$$

where I_{ex} is the expected signal evaluated from eq (1) with the current f(T) approximation, I_{ob} is the observed signal, m is the number of observations, w_i is a proper weight and λ is a Lagrange multiplier.

The best solution f_j is obtained from the conditions $\frac{\partial F}{\partial f_j} = 0$:

$$ln\ f_j = ln\ w_j - 1 - 2\lambda\Sigma_s \frac{(I_{ex,s} - I_{ob,s})^2}{\sigma_s^2} \frac{\partial I_{ex,s}}{\partial f_j}$$

Assuming $w_j = e\ f_j$ (old) and a trial value for the first f_j (old), the equation provides a very quick iterative procedure to get a new approximation f_j (new); the procedure converges since when $I_{ex} = I_{ob}$ the old and the new f_j are the same, and the

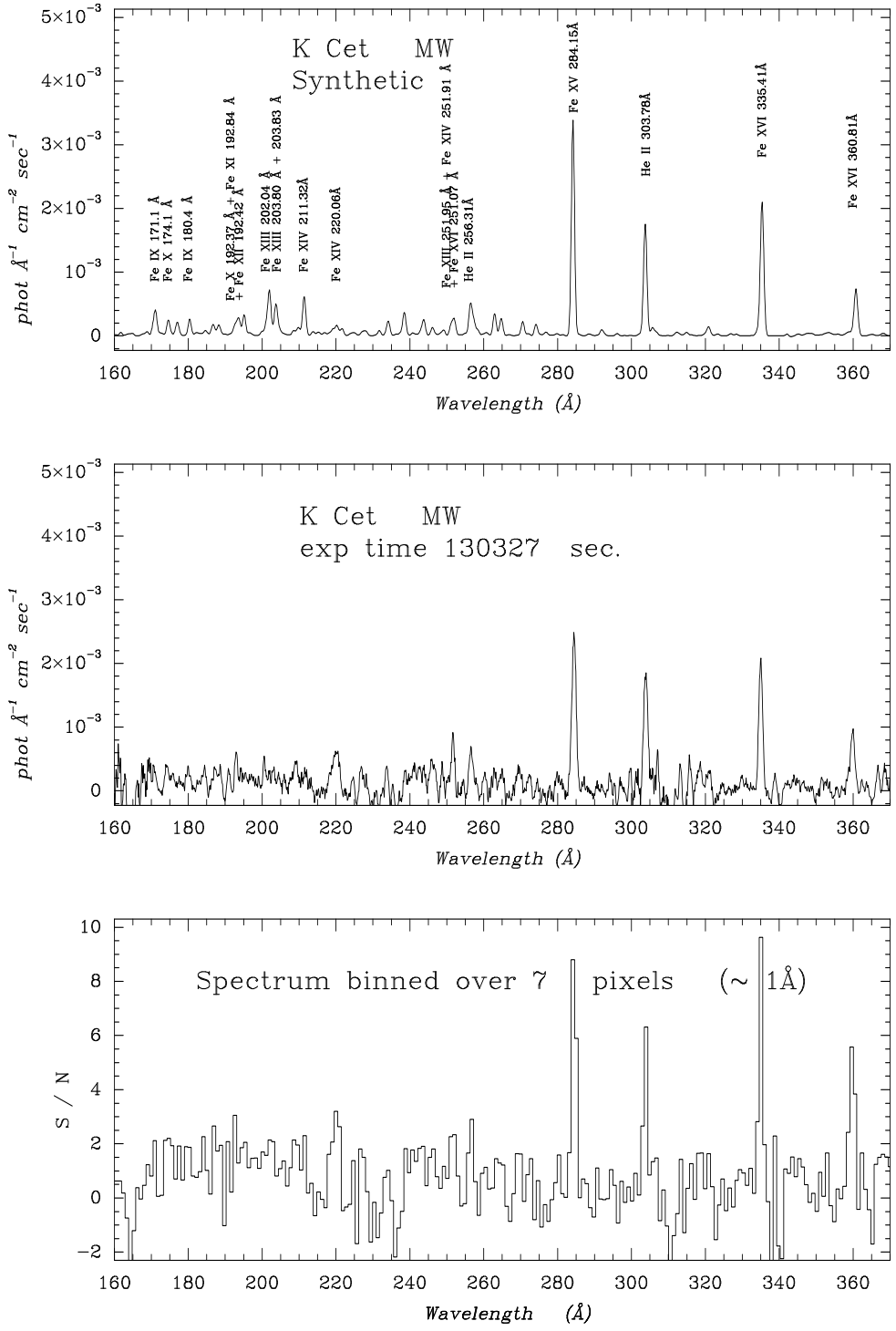

Fig. 3. The synthetic spectrum for the MW section *(Top)* is compared with the observation *(Middle)*.The signal to Noise ratio is shown in the *Bottom*

velocity of the convergence may be controlled by proper use of the Lagrange multiplier.

The smoothness of the DEM distribution depends on the number of selected mesh points (n). Large indetermination in the best solution occurs in those temperature intervals where poor constraints are put by the available observations. The solution is optimally constrained near log T = 5.0 and 6.0$\leq$ log T $\leq$ 7.0. This procedure has the advantage to give only positive f_j values (a rather important physical constraint), and proves to be quickly converging.

This numerical method has been applied to the lines listed in Table 1. The resulting Differential Emission Measure is shown in Fig. 2. For each line used in the DEM procedure a point is plotted in Fig. 2 at the temperature where the line is formed and at the DEM value necessary to fit the observations. It is worth

noting that most of the lines are fitted by the DEM within the error bars.

This function has a maximum near 3.2 10^6 K, typical of the quiescent phases of this kind of stars and of active regions of the Sun.

Some more comments are needed:

- The low temperature behavior ($logT \leq 5.4$) is dominated by the IUE lines, though the two He II lines are in reasonable agreement with them, taking into account that the IUE observation is not contemporary and despite the fact that the 303.8 line appears to be rather weak in comparison with other cool stars.
- The Fe XII 192 Å line receives significant contributions from the O V 2s2p ^{3}P - 2s3d ^{3}D multiplet.
- The Fe XIV line at 220 Å reveals a far too high observed flux, also including possible blendings.
- The Fe XV line at 284 shows a rather high theoretical flux, though it is possible to reproduce the observed value within its experimental uncertainties.
- Not all the lines measured by two of the three detectors have been used, but only one line for each couple has been kept. We decided to retain the MW value in order to use the same detector and avoid possible intercalibration uncertainties.
- Some IUE lines (C I, O I, Si II) have not been included in the calculation of the Differential Emission Measure because the evaluation of G(T) functions may have problems for temperature lower than 3.0 $10^4 K$ and optically thin assumption for these lines are probably unreasonable.

4. Synthetic spectra and further line identification

Using the DEM model shown in Fig. 2 and the new version of the Arcetri Spectral Code (Landi and Landini 1997) we have computed the synthetic spectrum of κ Cet for the wavelength range covering all the three channels of the EUVE spectrometer. The results are shown in Fig. 3 for the MW section and Fig. 4 for the LW section.

Through a comparison between the calculated synthetic spectrum and the observed one we are able to make some further identification of those lines whose intensity was too low to allow an easy identification as for the lines listed in Table 1. Only lines whose S/N ratio is greater than 2 have been considered.

In the Short Wavelength range no feature exceeds the S/N ratio equal 2. However the two lines Fe XVIII 103.937 and Fe IX 180.408 are predicted by the synthetic simulation; they could be present in the observed spectrum with S/N ratio slightly larger than 1. *Hotter* lines (Fe XXI 128.736 for example), often seen in stars during strong flare activity (Monsignori Fossi and Landini 1994a, Monsignori Fossi et al. 1995a, Monsignori Fossi et al. 1995b), show extremely low S/N ratios and their weakness confirms that κ Cet was in a quiescent phase during the time of the observation.

The Fe IX line at 180 can be identified also in the Medium Wavelength range. Other weak MW lines are Fe XIV 211.320, Fe XVI 251.074+Fe XIII 251.955+Fe XIV 252.910 and Fe XIII 203.80+203.83. The theoretical flux for the latter line is a bit too large and probably we could have matched better its experimental value lowering the assumed electron density of the emitting plasma. Nevertheless the constraint imposed by the Fe XII line at 192 Å did not allow us to lower N_e.

Table 2. Weak lines identified using the DEM model calculated in the present work. The three lines near 252 and the two O III lines near 508 are blended in the observed spectrum.

Ion	λ_{theor} (Å)	Log T	Detector
Fe XVIII	103.937	6.8	SW
Fe IX	180.408	5.8	SW and MW
Fe XIV	211.320	6.3	MW
Fe XVI	251.074	6.4	MW
Fe XIII	251.955	6.2	MW
Fe XIV	252.910	6.3	MW
O III	374.2	5.2	LW
O III	507.8	5.2	LW
O III	508.2	5.2	LW
O III	525.8	5.2	LW
SiXII	499.4	6.2	LW
SiXII	520.7	6.2	LW

For the LW section (Fig. 4) a number of features exceeds the S/N ratio equal 2 and are marked by " # " in the observed spectrum (Fig 4 middle). All but one have a counterpart in weak features of the synthetic spectrum that are labeled with the contributing wavelengths. As expected some of them are second order contribution, but O III 374.2 Å , 507.8Å +508.2 Å and 525.8 Å and SiXII 499.4 Å and SiXII 520.7 Å are probably detected at S/N = 2 and ArXVI 390.9 Å and NeIV 469.8 Å are only slightly out in wavelength.

5. Comparison with the solar spectrum

κ Cet is a solar-like star and its spectrum is expected to be similar to that of the Sun, though the much weaker signal coming from this star limits the comparison of the spectral features only to the most prominent lines. Differences between the two observed spectra may be due to important characteristics of the κ Cet emitting plasma, and may impose some constraint on the abundances of some elements relative to those of the Sun. For this reason a comparison between the EUV spectra of this two stars may be interesting.

In order to do such a comparison a spectrum measured with the Coronal Diagnostic Spectrometer (CDS) from the SOlar Heliospheric Observatory (SOHO) has been used. The spectrum concerns the total counts integrated over a slit covering a 4 $\times$ 240 $arcsec^2$ and including an Active Region on the Sun, under

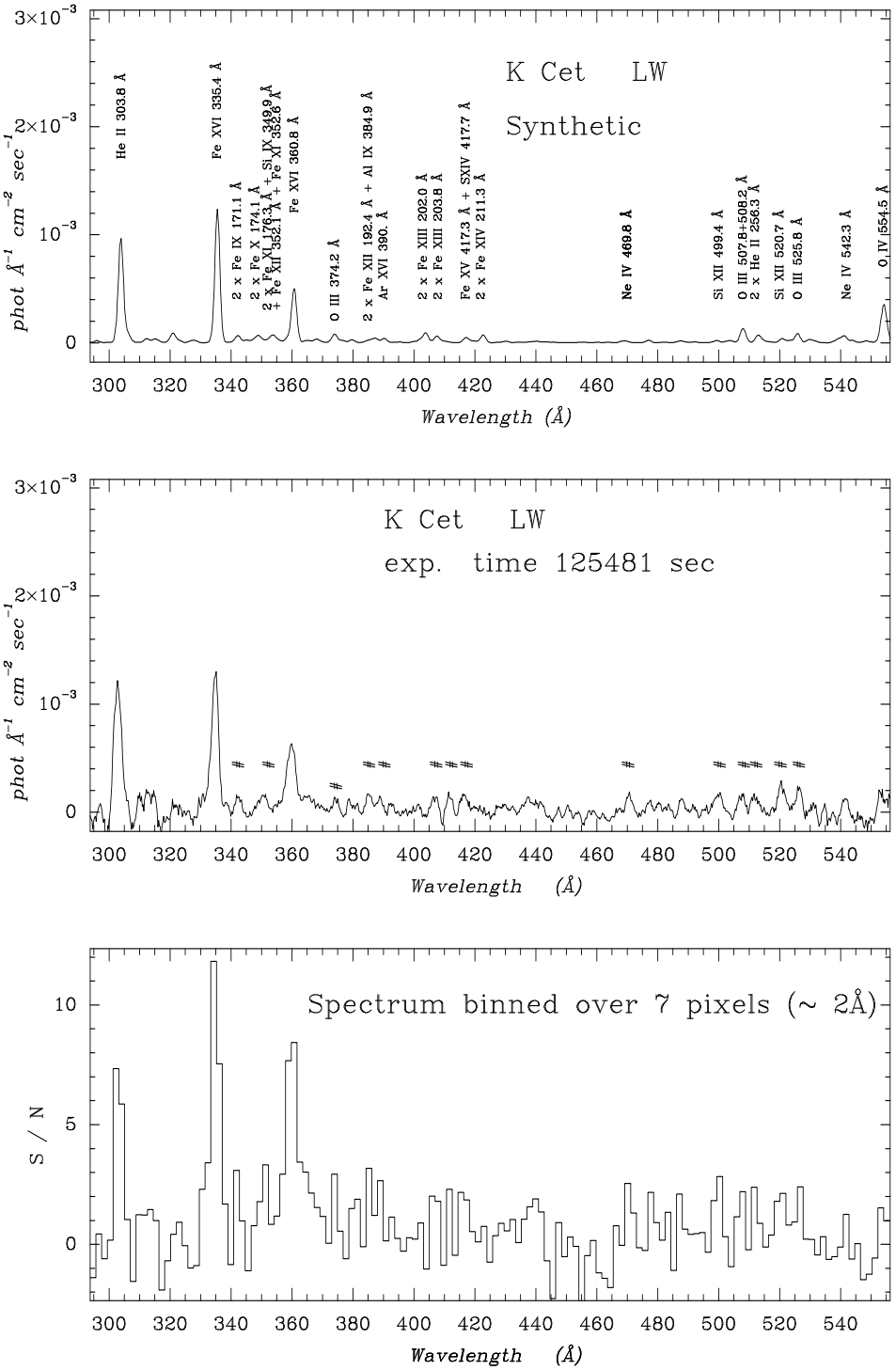

Fig. 4. The LW synthetic spectrum (top), the LW observed spectrum (middle) and the Signal-to-Noise ratio (bottom) plotted versus wavelength. Since wavelengths greater than 550 Å are mainly second order we have omitted that portion of the spectrum. Features in the synthetic spectrum are labeled with contributing lines. Features detected with S/N ratio better than 2 are marked "#" in the observed spectrum

conditions similar to those expected in κ Cet during the time of the EUVE observation.

The instrument and its performances are described in Harrison et al. 1995.

The CDS spectrometers have 6 spectral windows that cover a spectral range from 151 to 785 Å , similar to that of EUVE SW, MW and LW channels. Nevertheless, since the EUVE LW channel is strongly affected by interstellar absorption, and that the SW spectral range is only marginally observed by CDS, we restrict our comparison only to the CDS Normal Incidence (NIS) channel 308-381 Å and to the Grazing Incidence (GIS) channels 151-221, 256-338. A composite solar spectrum is produced and comparison with MW EUVE section is shown in Fig. 5.

The GIS-1 solar spectrum covers the spectral range 151-221 Å . The most prominent lines are Fe IX 171.1, Fe X 174.5, Fe X 177.2 and Fe XII 188.2 Å . The first two spectral features have

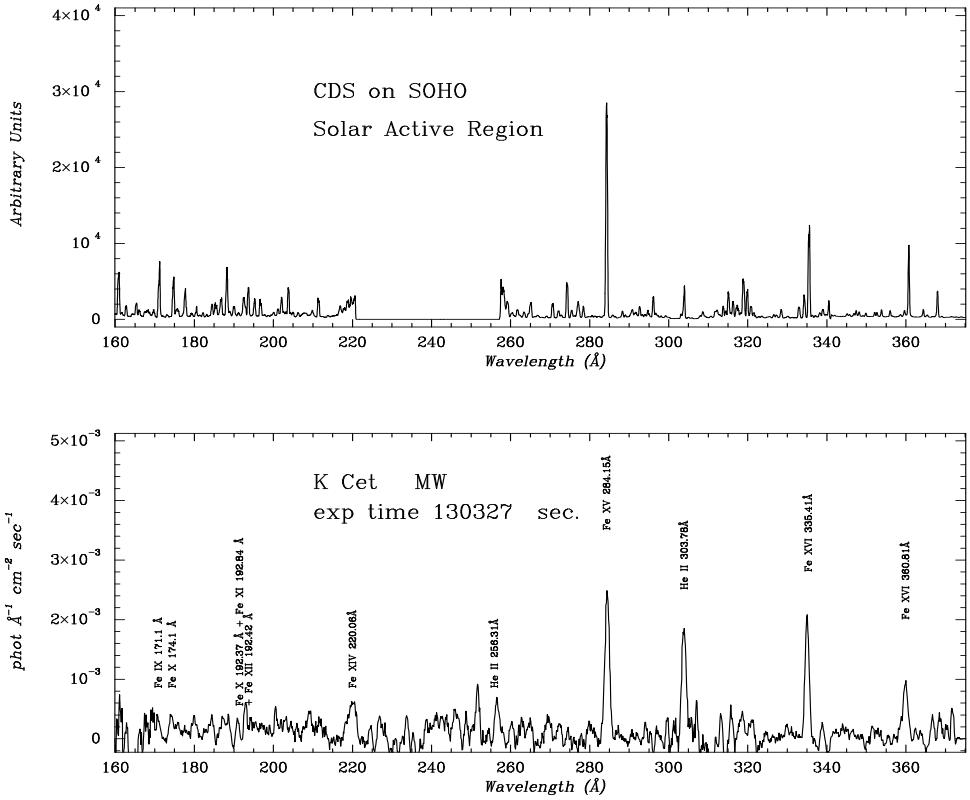

Fig. 5. The MW spectrum of κ Ceti *(Bottom)* is compared with CDS-SOHO spectrum of a Solar Active Region *(Top)*. The He II 303.8 line has been suppressed in the solar spectrum.

been identified in both the EUVE SW and MW spectrometers and have been used in the calculation of the model of Differential Emission Measure of κ Cet. Line Fe X 177.2 Å cannot be identified with confidence in the SW spectrometer since it lies in a very noisy part of the SW spectrum. Fe XII 188.2 Å line is not visible in the MW spectrum. The MW line at 192 Å , composed by a blend of Fe XII, Fe X and Fe XI lines, is much weaker than the other observed GIS-1 lines, while it has been identified and used in our study of EUVE spectrum. As in the EUVE spectrum, the two strongly density dependent Fe XIII lines around 203 Å are much weaker than the other lines. Unfortunately the 220 Å line lies at the extreme limit of the GIS-1 spectral range and cannot be compared with the MW line.

The GIS-2 spectrum lies in the range 256-338 Å and is largely dominated by the Fe XV 284.15 Å line and the Fe XVI 335.4 Å line. This two lines are the strongest lines in the K Cet spectrum and have been used for the DEM study. Their intensities are roughly in the same ratio as in the EUVE observation, though in the latter the Fe XVI line appears to be weaker.

The He II 303.8 Å line is artificially removed from the CDS spectrum. The Fe XIV 274 Å line in the solar spectrum lies in the noise of the MW channel. Also the spectral region 310-320 Å , rich of Fe XIII, Si VIII and Mg VIII lines seen in the solar spectrum, lies in the noise of the spectrum of K Cet.

The NIS-1 spectrum covers the range 308-381 and is dominated by the two strong Fe XVI lines 335 and 360 Å . They are clearly seen in both the MW and LW spectrum and their fluxes have been used for the DEM calculation. Their EUVE intensity ratio, when corrected for interstellar absorption, is nearly identical to the solar one and this is a further evidence that the assumed column density N_H=2 10^{18} cm^{-2} for K Cet is a reasonable value. The strong Mg IX line at 368 Å is clearly visible in the solar spectrum while it is nearly absent in both the LW and MW channels. Its solar intensity suggests that it should be identified in the EUVE observation, unless the K Cet abundance for Magnesium is smaller than the solar one.

The GIS-3 solar spectrum (393-493 Å) does not show any strong line, accordingly to the LW observation which is very flat.

The comparison between the K Cet EUVE spectrum and a solar Active Region observed with the SOHO-CDS spectrometers has outlined the following features:

- The two spectra are very similar, especially for the strongest lines of the spectrum.
- There could be some differences in the abundances of Silicon and Magnesium relative to Iron since some relatively strong solar lines are not visible in the EUVE spectrum.
- A longer exposure time of K Cet could have helped in identifying several weaker lines observed in the solar spectrum which could allow to evaluate the electron density of the emitting source, and to verify the abundances of the elements.

6. Conclusions

We have analyzed the EUV spectrum of the solar-like star κ Cet (HD 20630) observed with the SW, MW and LW spectrometers of the EUVE satellite. We have measured the fluxes of the

strongest lines of the spectrum and we have calculated a model for the Differential Emission Measure of the source. Since we are interested in developing a DEM model of the Transition region as well as for the corona of K Cet we have complemented the EUVE observed fluxes with the observation of this star carried on with the IUE spectrometer in the range 1200-1800 Å . The analysis of these two spectra has led to the calculation of the DEM model, to put some constraint on the electron density of the emitting source and to a critical discussion of some IUE and EUVE observed fluxes. Using the derived Differential Emission Measure the synthetic spectrum has been calculated, and the identification of a few weak lines has been possible. The spectrum of κ Cet happens to be very similar to that measured by the Coronal Diagnostic Spectrometer on SOHO looking at a Solar Active Region.

Acknowledgements. We want to acknowledge and remember Brunella Monsignori-Fossi, who so early and suddenly died at the beginning of 1996; she was Guest Investigator in the EUVE Observations of K Cet and deeply involved in the development of the Arcetri spectral code and in the CHIANTI database assessment.

References

Arnaud M., Raymond J., 1992, ApJ, 398, 394
Bowyer S., Malina R.F., 1991, Extreme Ultraviolet Astronomy, eds. R.F. Malina, S. Bowyer, Pergamon Press, New York
De Castro E., Fernández-Figueroa M.J., Rego M., Ponz D., 1981, A& A, 102, 207.
Dere K.P., Landi E., Mason H.E., Monsignori Fossi B.C., Young P.R.,1996, A& AS, in press
Fernández-Figueroa M.J., De Castro E., Rego M., 1981, A& A, 99, 141
Harrison R. et al., 1995, Sol. Phys., 162, 233
Jeffrey C.S., Rosner R., 1986, ApJ, 310, 463
Jordan C., 1969, MNRAS, 142, 501.
Jordan C., 1992, Mem. Soc. Astr. It., 63, 605.
Jordan C., Montesinos B., 1991, MNRAS 252, 21
Jordan C., Brown A., Walter F.M., Linsky J.L., 1986, MNRAS, 218, 465
Landi E., Landini M.,1997, *The Arcetri spectral code for EUV emission lines*, in preparation
Landini M., Monsignori Fossi B.C, 1990, A& AS, 82, 229
Landini M., Monsignori Fossi B.C, 1991, A& AS, 91, 183
Landini M.,Monsignori Fossi B.C.,Paresce F,Stern R.A.,, 1985, ApJ, 289, 209
Monsignori Fossi, B.C., Landini M., 1991a, Adv.Space.Res, 11, 281
Monsignori Fossi, B.C., Landini M., 1991b, in *Intensity Integral Inversion Techniques: a study for SOHO mission*, eds R.A. Harrison, A.M. Thompson, Rutherford Appleton Laboratory Report, RAL-91-092, 27
Monsignori Fossi B.C., Landini M., 1994a, A& A, 284, 900
Monsignori Fossi B.C, Landini M., 1994b, Sol. Phys, 152, 81
Monsignori Fossi B.C., Landini M., Pallavicini R., Tribioli F., 1986, Adv.SpaceRes., 6, 8, 137
Monsignori Fossi B.C., Landini M., Drake J.J., Cully S.L.,1995a, A& A, 302, 193
Monsignori Fossi B.C., Landini M., Fruscione A., Dupuis J., 1995b, ApJ, 449, 376
Oranje B.J., 1986, A& A, 154, 185
Pallavicini R., Monsignori Fossi B.C., Landini M., Schmitt J.H.M.M., 1988, A& A, 191, 109
Paresce F., 1984, ApJ, 89, 1022
Rego M. , Fernández Figueroa, M.J., 1979, A& A, 76, 249
Rego M., Cornide M. and Fernández Figueroa M.J. , 1980, A& AS, 39,251
Robinson R., Bopp B.W.,1987, 5th Workshop on Cool Stars, p.291
Rumph T., Bowyer S., Vennes S., 1994, ApJ, 107, 2108
Rutten R.G.M., 1987, A& A, 177, 131
Saar S.H., 1987, PhD thesis, University of Colorado.
Saar S.H. and Baliunas S.L., 1992, in "The solar cycle" ASP Conf Series, Vol 27 (ed K.L. Harvey), p.197
Saar S.H., 1990, in The Solar Photosphere: Structure, Convection, Magnetic Fields (Ed. J.O. Stenflo) Kluwer, Dordrecht, p.427
Schmitt J.H.M.M., Pallavicini R., Monsignori-Fossi B.C., Harnden F.R., 1987, A& A, 179, 193
Zirin H. 1976, ApJ, 208, 414

This article was processed by the author using Springer-Verlag LaTeX A&A style file *L-AA* version 3.